Electronic and Magnetic Properties of Metal-(4,4 '-bipyridine) Sandwich Complexes and Their Nanowires

ARTICLE *in* THE JOURNAL OF PHYSICAL CHEMISTRY A · JANUARY 2011

Impact Factor: 2.69 · DOI: 10.1021/jp110442x · Source: PubMed

2 AUTHORS:

Anup Pramanik
Visva Bharati University
27 PUBLICATIONS **98** CITATIONS
SEE PROFILE

Hong Seok Kang
Jeonju University
76 PUBLICATIONS **1,385** CITATIONS
SEE PROFILE

Electronic and Magnetic Properties of Metal−(4,4′-bipyridine) Sandwich Complexes and Their Nanowires

Anup Pramanik[†] **and Hong Seok Kang***[,‡]

Institute of Engineering Research and Department of Nano and Advanced Materials, College of Engineering, Jeonju University, Hyoja-dong, Wansan-ku, Chonju, Chonbuk 560-759, Republic of Korea

Received: November 1, 2010; Revised Manuscript Received: November 29, 2010

Using calculations based on density functional theory, we have investigated the geometric, energetic, and magnetic properties of complexes of 4,4′-bipyridine (BPY) with metal atoms M (= Li, V, and Ti). The systems of interest include BPY−M_2 and BPY_2−M_2 complexes and $(BPY-M_2)_x$ nanowires in which the sandwich structure is stacked infinitely along one direction. For each of these systems, a detailed analysis was performed on the electronic structure. First, we found that BPY−M (M = V and Ti) binding is stronger than BPY−Li binding because of the covalent nature of the former interaction. The difference in the magnetic properties of BPY−M_2 and BPY_2−M_2 (M = V and Ti) complexes can be understood in terms of the different strengths of the M−M interactions mediated by d(M) or sd(M)-hybridized orbitals. Second, we found that the $(BPY-Li_2)_x$ nanowire is a semiconductor, whereas $(BPY-V_2)_x$ and $(BPY-Ti_2)_x$ nanowires are magnetic metals due to the spin-polarization in d_z2(M)-derived bands.

1. Introduction

Recently, there has been great interest in complexes composed of neutral metal atoms and aromatic molecules and their infinite 1D crystals or nanowires. The first class of these systems is Li−R complexes, where R = benzene, naphthalene, pyrene, or graphite. Calculations on those systems reveal that these aromatic molecules are good Li storage materials.[1,2]

The second class includes a large number of complexes involving transition-metal atoms instead of Li, which has been extensively investigated since the gas-phase synthesis of organometallic complexes using the laser vaporization technique.[3−5] Particular attention has been paid to vanadium complexes because mass spectra showed that it had the largest tendency to form multiple deckers with benzene among all 3d transition metals investigated.[6] In particular, the 1D nanowire of the benzene−vanadium sandwich complex was shown to be half-metallic, that is, 100% spin-polarized.[7,8] In another work, the vanadium−benzene sandwich complex was shown to exhibit ferromagnetic spin coupling and a chiral confirmation at terminal units.[9] The ferrimagnetic spin coupling in the vanadium−naphthalene 1D nanowire results in a magnetic moment that is 45% larger than that of the vanadium−benzene 1D nanowire.[7] Very recently, carrier-tunable magnetic ordering has been found for the nanowire.[10] A density functional calculation revealed that TM−(ferrocene) 1D nanowire was shown to be ferromagnetic semiconductors, where TM = Ti, Sc, and V.[11]

These sandwich complexes can be very useful in spintronics because their spin-coherence distance and time are longer than those of conventional metal or semiconductor nanostructures. In this respect, there have been some theoretical investigations on quantum conductance through sandwich complexes, which have shown interesting properties like spin-filtering and negative differential resistance.[12]

Therefore, it is important to investigate the electronic and magnetic properties of sandwich complexes involving aromatic molecules other than those previously investigated. In this work, we will focus on 4,4′-bipyridine (BPY) complexes with metal atoms M (= Li, V, and Ti) using calculations based on density functional theory. It is known that Ti prefers sandwich complexes to rice-ball structures in which the metal clusters are fully covered with benzene molecules.[13] Li is a simple metal without d electrons, and its mass storage is of industrial importance for use in Li batteries. BPY differs from naphthalene in that there is a single bond between the two aromatic rings.

2. Theoretical Methods

Geometry optimizations for the individual molecules and for their complexes were performed using the Vienna ab initio simulation package (VASP).[14] Electron−ion interactions were described by the projector-augmented wave (PAW) method,[15] which is basically a frozen-core all-electron calculation. The exchange-correlation was treated within the generalized gradient approximation proposed by Perdew, Burke, and Ernzerhof (PBE).[16] For structure optimization, atoms were relaxed toward the direction of the Hellmann−Feynman force using the conjugate gradient method until a stringent convergence criterion (0.03 eV/Å) was satisfied. For vanadium, all of the 3d electrons were treated as valence electrons. For nanowires, the lattice parameter along the crystal direction (*Z*) was optimized using eight *k*-points in the irreducible region of the first Brillouin zone. The optimal lattice parameter was chosen to give the minimum total energy with respect to changes in the parameter. The supercell parameters along the other two directions were kept sufficiently large so that the interatomic distances between neighboring cells were >11 Å.

3. Results

Let us first consider the formation of the Li−BPY complex in two steps, BPY + 2Li (doublet) → BPY−Li_2 (singlet) and BPY−Li_2 (singlet) + BPY → BPY_2−Li_2 (singlet), which are

* Corresponding author. E-mail: hsk@jj.ac.kr.
[†] Institute of Engineering Research.
[‡] Department of Nano and Advanced Materials, College of Engineering.

10.1021/jp110442x
Published on Web 12/14/2010

TABLE 1: Binding Energies for the Two Processes: BPY + 2M → BPY−M_2 and BPY−M_2 + BPY → BPY_2−M_2[a]

M	E_b^1 (eV)	E_b^2 (eV)	$E_b^1 + E_b^2$ (eV)
Li	−2.48 (−2.23)	−1.95 (−1.40)	−4.43 (−3.63)
V	−4.44 (−4.64)	−5.01 (−4.59)	−9.45 (−9.23)
Ti	−6.18 (−6.35)	−4.33 (−4.23)	−10.51 (−10.58)

[a] Numbers in parentheses denote the corresponding values for the complex involving Np instead of BPY.

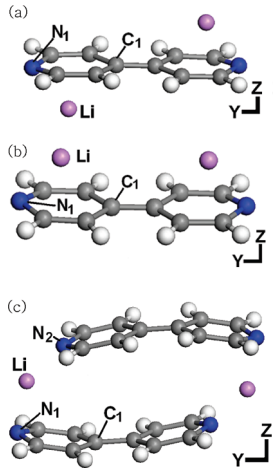

Figure 1. Optimized geometries of **BPY−Li_2** for (a) anti and (b) syn configurations and (c) **BPY_2−Li_2** sandwich complex.

defined as P1 and P2 with binding energies of E_b^1 and E_b^2, respectively. For BPY−Li_2, we find that the anti configuration in which the two Li atoms are located on opposite sides of the BPY plane is 0.09 eV more stable than the syn configuration, in which they are located on the same side. We recall that a similar observation was also made for the Np−Li_2 complex, where Np is naphthalene.[2] Therefore, we assume that one of the two Li atoms rearranges itself from the anti configuration in such a way that it comes into the interplanar region of the two BPY molecules in process P2.

Table 1 shows that the binding energy for each of the two processes is appreciably larger than that involving Np molecules instead of BPY molecules quoted in ref 2, indicating a better Li-storage capacity of BPY than that of Np. Specifically, the large negative value (= 1.95 eV) of E_b^2 indicates that the sandwich formation is indeed possible. In an isolated BPY molecule, the two pyridine rings are not coplanar, and the dihedral angle around the single bond between the two pyridine rings is 42.6°, which is in reasonable agreement with the experimental value (37.2°) from an electron diffraction experiment.[17] Upon Li adsorption resulting in BPY−Li_2, however, Figure 1 shows that the two rings become planar regardless of their configuration. Li atoms are located on top or bottom of the pyridine rings in such a way that they are slightly (∼0.15 Å) shifted from the center of the rings toward the terminal nitrogen atoms. Table 2 shows the various structural parameters for the two configurations. Specifically, the distance from a Li atom to the plane of a pyridine ring, *l*(Li-R), is 1.67 and 1.64 Å for anti and syn configurations of BPY−Li_2, respectively. A separate analysis of the electronic structure shows that the HOMO-1 and HOMO of BPY−Li_2 correspond to the HOMO and LUMO of BPY, whereas the LUMO is mostly derived from 2s(Li) with a minor contribution from the LUMO+1 of BPY. This observation clearly indicates a transfer of nearly two electrons from 2s(Li) to BPY, resulting in the formation of the BPY^{2-}−Li_2^+ ionic complex. As a result, the HOMO−LUMO gap decreases from 3.26 to 0.58 eV upon complex formation. We can also understand the higher stability of the anti configuration of BPY−Li_2 in terms of the weaker electrostatic repulsion between Li^+ ions compared with the syn configuration.

In BPY_2−Li_2 sandwich complex, which is characterized by C_{2h} symmetry, Figure 1c shows that the BPY molecules are slightly bent toward the Li atoms, and one of the two BPY molecules is offset from the other in such a way that the Li atoms are located above the terminal nitrogen atoms of the BPY. In addition, Li atoms are located outside the pyridine ring (= R_2) in which N_2 atom belongs, indicating that the major contribution to Li−R_2 interaction is the electrostatic interaction between Li and N_2. This result is clearly different from the case of the Np_2−Li_2 sandwich complex, which has D_{2h} symmetry with both Li atoms inside benzene rings when viewed along the crystal axis.[2]

We have also studied the infinite 1D nanowire of the $(BPY-Li_2)_x$ system. Figure 2 shows the structure of this system. Its magnetic moment is zero and binding energy (E_b^c) is as much as −4.74 eV, which is defined for the process BPY + 2Li (doublet) → $(BPY-Li_2)_x$ nanowire. A comparison of this value with E_b^1 (−2.48 eV) in Table 1 indicates that the wire formation indeed stabilizes the complex to a significant degree. In the nanowire, the optimal lattice constant along the *Z* axis is 4.10 Å, and the two pyridine rings in the BPY molecule are almost coplanar and tilted by 25° with respect to the *Y* axis. Therefore, the interplanar distance between two BPY molecules is 3.96 Å, which is appreciably shorter than that (= 4.13 Å) between the two BPY molecules in the BPY_2−Li_2 sandwich complex. The tilted configuration can be ascribed to the fact that two Li atoms are adsorbed on a BPY molecule in anti conformation,

TABLE 2: Geometric Parameters, Spin Multiplicity (2S+1), and Binding Energy (E_b^1) for BPY−M_2 and BPY_2−M_2, Where *M* = Li, V, and Ti[a]

	BPY−Li_2		BPY−V_2		BPY−Ti_2				
configs.	anti	syn	syn	anti	syn	anti	BPY_2−Li_2	BPY_2−V_2	BPY_2−Ti_2
$l(N_1\text{-M})$	2.04	2.01	2.14	2.01	2.19	2.13	1.98	2.17	2.19
$l(C_1\text{-M})$	2.35	2.38	2.12	2.15	2.22	2.28	3.43	2.25	2.31
l(M-R)[b]	1.67	1.64	1.54	1.49	1.74	1.61	1.98	1.67	1.72
$l(N_2\text{-M})$							1.94	2.18	2.19
l(M-M)	5.80	4.47	3.06	5.34	2.86	5.58	8.18	4.49	4.79
l(R-R)[c]							4.13	3.33	3.24
2S+1	1	1	5	3	5	3	1	3	1
E_b^1	−2.48	−2.39	−4.44	−3.83	−6.18	−4.95	−1.95[d]	−5.01[d]	−4.33[d]

[a] Atomic labels are defined in Figures 1, 4, and 9. [b] Distance between a Li atom and the pyridine plane of a BPY molecule. [c] Inter-BPY distance in BPY_2−M_2 sandwich complex. For BPY_2−Li_2, it is defined as the distance along the *Z* axis between C−C single bonds belonging to different BPY molecules. [d] E_b^2 defined for process P2.

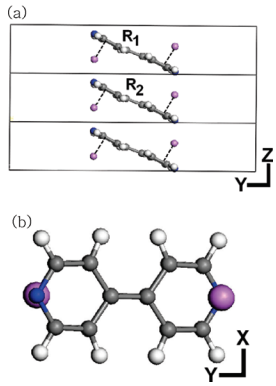

Figure 2. One-dimensional crystal structure of $(\mathbf{BPY-Li_2})_x$ system, projected onto (a) **YZ** and (b) **XY** planes.

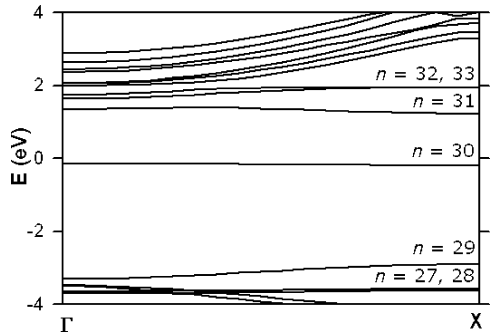

Figure 3. Band structure of $(\mathbf{BPY-Li_2})_x$**1D** crystal.

not syn conformation, which has also been shown to the case for the BPY_2-Li_2 sandwich complex. l(Li−R) (= 1.80 Å), that is, the closest distance between a Li atom and the closest pyridine ring (= R_1), is appreciably shorter than that (= 1.98 Å) of the BPY_2-Li_2 sandwich complex, as shown in Table 2.

The band structure in Figure 3 shows that this wire is a semiconductor with a band gap of 1.42 eV. As indicated in the Figure, the valence (n = 30) and conduction (n = 31) bands are exclusively derived from the LUMO and LUMO+1 of BPY molecule, respectively. As expected from our analysis of the BPY−Li_2 complex, this observation clearly indicates that there is a transfer of two electrons from the two Li atoms to BPY, forming an ionic $(BPY^{2-}Li_2^{+})_x$ system. In these bands, the electron densities on the lithium atoms are nearly zero because the 2s(Li) level lies far above. As a result, these bands show almost no dispersion in the plot of E versus k, being even flatter than those of the $(Np-Li_2)_x$ nanowire.[2] Therefore, the conductivity of the electron or hole along the wire direction will be quite small.

As indicated in Table 1, the binding strength is far greater for vanadium complexes. For the $BPY-V_2$ complex, the syn configuration shown in Figure 4a is more stable than the anti configuration shown in Figure 4b by 0.61 eV, which is much larger than the energy difference for the two configurations of the BPY−Li_2 complex. Table 2 shows the various structural parameters. l(V−R) (= 1.54 and 1.49 Å for the syn and anti configurations, respectively) is shorter than the corresponding distance in the BPY−Li_2 complex. Consistent with this observation, the inter-BPY distance (= 3.33 Å) of the BPY_2-V_2 sandwiched complex is also shorter than that (= 4.13 Å) of the BPY_2-Li_2 complex. In addition, the interatomic distance (= 3.06 Å) between V atoms in the syn complex along the Y axis is noticeably shorter than that (= 4.47 Å) in the syn complex of BPY−Li_2, indicating the possible formation of a bond between the V atoms via the bending of BPY molecule.

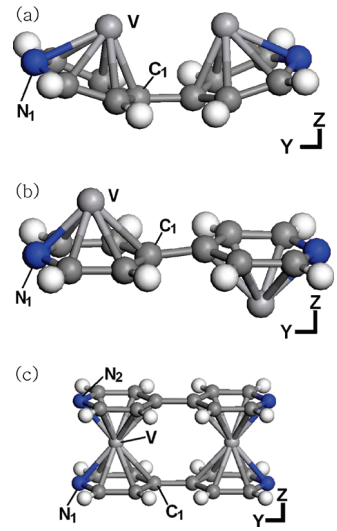

Figure 4. Optimized geometries of $\mathbf{BPY-V_2}$, for (a) syn and (b) anti configurations and (c) $\mathbf{BPY_2-V_2}$ sandwich complex.

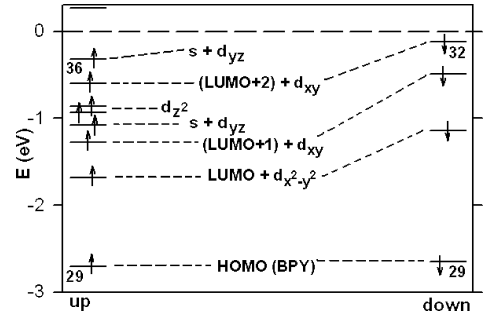

Figure 5. Energy level diagram of *syn* configuration of $\mathbf{BPY-V_2}$ for spin-up (left) and spin-down (right) states.

This conjecture is borne out by our electronic structure analysis, shown in Figure 5. Two (n = 30 and 31) of the 10 d orbitals from the two vanadium atoms are completely filled with spin-pairing. The most efficient bonding overlap of two d orbitals along the Y axis from each V atom of the syn configuration is achieved by the $d_x2_{-y}2$ orbital, which is the case for n = 30. A slightly less efficient bonding overlap with a slightly higher energy level is accomplished by d_{xy}, which is the case for n = 31. In addition, these two orbitals are hybridizations of d orbitals with the appropriate molecular orbitals (MOs) of BPY through symmetry-allowed interactions, that is, LUMO and LUMO+1, respectively. The antibonding interaction (= 35↑ and 32↓) of the two d_{xy}(V) orbitals, also hybridized with LUMO+2 of BPY is also spin-paired. The aforementioned value of l(V−R), shorter than that in BPY−Li_2 manifests such hybridization. In other words, the V−BPY interaction is partially covalent, whereas the Li−BPY interaction is almost ionic. Only four spin-up states (= 32↑ ∼ 34↑ and 36↑) are filled in the other four d-derived orbitals, that is, d_{yz}^{B}(V), d_z2^{B}(V), d_z2^{A}(V), and d_{yz}^{A}(V), since each of them is derived from bonding (= B in superscript) or antibonding (= A in superscript) combination of $d_\alpha(V_1)$ and $d_\alpha(V_2)$ orbitals, which do not exhibit an appreciable overlap with each other, resulting in quintet state [$\alpha = yz$ and z^2]. In addition, the state (= 32↑) derived from the d_{yz}^{B}(V) orbital hybridizes with 4s(V) orbital through sd-hybridization, further strengthening the V−V bond. In short, the syn configuration becomes more stable than the anti configuration of the $BPY-V_2$ complex because of intervanadium covalent interactions, which can also explain the high spin state of the system.

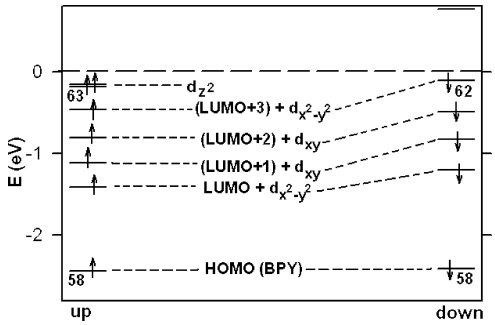

Figure 6. Energy level diagram of $\mathbf{BPY_2-V_2}$ sandwich complex for spin-up (left) and spin-down (right) states.

Next, we describe our results for the BPY_2-V_2 sandwich complex. We find that the magnitude of E_b^2 (= −5.01 eV) in Table 1 is larger for BPY_2-V_2 than that (= −4.59 eV) of Np_2-V_2, indicating easier sandwich formation compared with the Np system. It is worth noting that the intervanadium distance (= 4.49 Å) of the complex is significantly longer than that of the BPY−V_2 (= 3.06 Å) or the Np_2V_2 (= 2.70 Å) sandwich complex. These two observations suggest that the energy gain from the η^6 BPY−V interaction more than compensates for the energy loss due to the significant weakening of the V−V bonding. Because the Np−V interaction in the Np_2V_2 sandwich is also η^6, these observations also indicate that the η^6 interaction is appreciably stronger in BPY_2-V_2. In fact, the inter-ring distance (= 3.33 Å) of BPY_2-V_2 sandwich shown in Table 2 is shorter than that (= 3.60 Å) of the Np_2V_2 sandwich.

The longer intervanadium distance of BPY_2-V_2 suggests that the overlap between the $d(V_1)$ and $d(V_2)$ orbitals is much less effective than in BPY−V_2 or Np_2-V_2, resulting in a smaller difference in energy between the two levels derived from their bonding and antibonding interactions. For example, n = 59 and 62 in Figure 6 correspond to the bonding and antibonding interactions of the $d_x2_{-y}2(V_1)$ and $d_x2_{-y}2(V_2)$ orbitals hybridized with LUMO and LUMO+3 of BPY, respectively, whereas n = 60 and 61 correspond to bonding and antibonding interactions of $d_{xy}(V_1)$ and $d_{xy}(V_2)$ orbitals hybridized with LUMO+1 and LUMO+2 of BPY, respectively. In addition, the spin-up and spin-down states of each of these levels exhibit exchange splitting smaller than that in BPY−V_2. For example, the splitting of n = 59 in Figure 6 is 0.21 eV, whereas the corresponding splitting of n = 30 in Figure 5 is 0.54 eV. This is because the effective space available to electrons in these levels is larger than that in BPY−V_2 because of the larger size of BPY_2-V_2. As a result, spin-paring is more enhanced in BPY_2-V_2. Two $d_z2(V)$-derived levels (n = 63 and 64) lie just above those spin-paired levels because the crystal field destabilizes $d_{xz}(V)$- and $d_{yz}(V)$-derived levels to a greater extent. In addition, the two levels are almost degenerate because the overlap of $d_z2(V_1)$ and $d_z2(V_2)$ orbitals governing their splitting is quite small in such a way that the splitting is smaller than the exchange splitting. Therefore, only spin-up levels are filled for them, resulting in a triplet state.

Figure 7 shows the geometric structure of the $(BPY-V_2)_x$ 1D nanowire. Its magnetic moment is 2.13 μ_B and also has a larger value (= −8.03 eV) of E_b^c with an optimized lattice parameter of 3.42 Å along the crystal axis. The lattice energy (= −3.59 eV) of the wire, which is defined as $E_b^c - E_b^1$ in Table 2, is appreciably more negative than that (= −2.26 eV) of $(BPY-Li_2)_x$ nanowire. This observation indicates that the formation of the former is easier than that of the latter. A comparison of the lattice energy with that (= −3.40 eV) of the

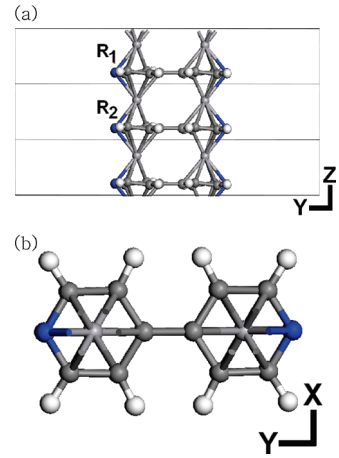

Figure 7. 1D crystal structure of $\mathbf{(BPY-V_2)_x}$ system, projected onto (a) **YZ** and (b) **XY** planes.

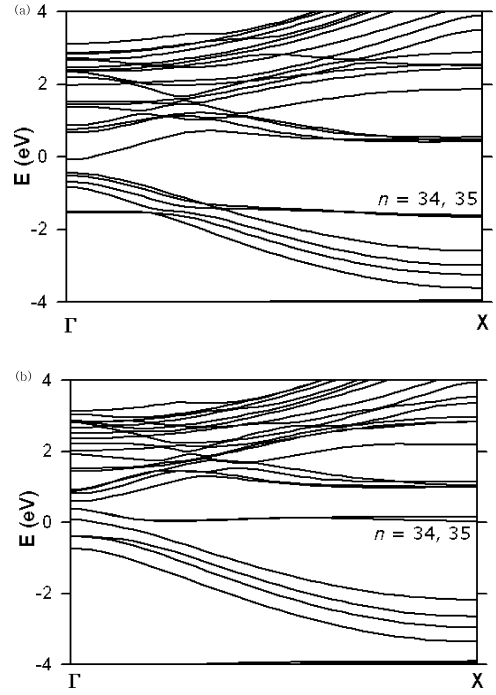

Figure 8. Band structure of $\mathbf{(BPY-V_2)_x}$**1D** crystal for (a) spin-up and (b) spin-down states.

$(Np-V_2)_x$ nanowire shows that the $(BPY-V_2)_x$ nanowire is also more stable than the $(Np-V_2)_x$ nanowire, which also seems to be due to the stronger η^6 interaction in the system involving BPY.[7]

The band structure shown in Figure 8 indicates that the wire will exhibit metallic behavior. As expected from our analysis on the BPY_2-V_2 sandwich complex, the bands around the Fermi level are subject to noticeable dispersion in the plot of E versus k because of the covalent nature of the π(BPY)−d(V) interaction. Meanwhile, the magnetism is mostly due to the large exchange splitting of nearly degenerate bands (n = 34 and 35 in Figure 8), which is derived from the bonding and antibonding interactions of the $d_z2(V_1)$ and $d_z2(V_2)$ orbitals. The flatness of those bands can be ascribed to the fact that these d orbitals cannot make a symmetry-allowed overlap with the σ(DPY) or π(DPY) states near the Fermi level. Namely, the lobes of these d orbitals directing toward centers of pyridine rings are nodeless (s-like) when viewed along the crystal axis, whereas the DPY states have many nodes (p-, d-, or f-like). This observation also indicates that the origin of the especially large exchange splitting

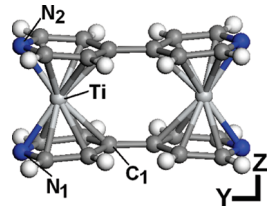

Figure 9. Optimized geometry of $\mathbf{BPY_2-Ti_2}$ sandwich complex.

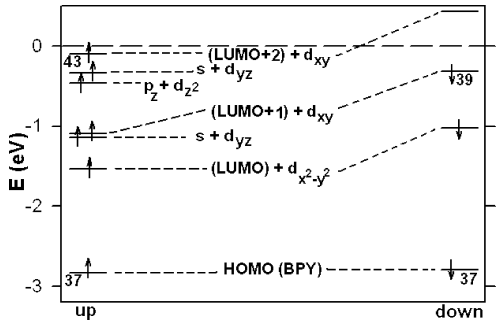

Figure 10. Energy level diagram of syn configuration of $\mathbf{BPY-Ti_2}$ for spin-up (left) and spin-down (right) states.

of those two bands is the confinement of the electrons exclusively around the vanadium atoms. The magnetic coupling between V atoms belonging to different unit cells is due to superexchange mediated by BPY molecules, which is manifested in opposite values of the local magnetic moment for V (= 1.21 μ_B) and BPY (= −0.15 μ_B), respectively. Meanwhile, spins of two V atoms belonging to the same unit cell interact via direct coupling, noting that spins of an isolated vanadium dimer separated by 4.49 Å also couple ferromagnetically.

Here we investigate BPY−Ti complexes. As indicated in Table 2, the binding of the syn configuration of $BPY-Ti_2$ is even stronger than that of $BPY-V_2$. In agreement with this observation, the Ti−Ti distance (= 2.86 Å) in the syn configuration is even shorter than the V−V distance (= 3.06 Å) in $BPY-V_2$. Upon formation of the sandwich complex, however, the distance becomes longer than that in BPY_2-V_2. Figure 9 shows that the BPY molecules adopt concave geometries in the sandwich complex. The Ti−Ti bonding can still be maintained despite the Ti−Ti distance being longer than the V−V distance in BPY_2-V_2 because d(Ti) orbitals are spatially more extended than d(V) orbitals. The sandwich complex is further stabilized by the electrostatic interaction of Ti ions with the BPY N atoms, whereas the electrostatic repulsion between the two N atoms is reduced by this peculiar geometry. When viewed along the Z axis, the Ti atoms are in fact shifted toward the N atoms in such a way that they are not located at the center of pyridine rings, unlike in the case of BPY_2-V_2. Comparison of the value (= −4.33 eV) of E_b[2] with that (= −4.23 eV) of Np_2-Ti_2 in Table 1 also shows that the distorted η^6 interaction is stronger than in Np_2-Ti_2, although it does not lead to the higher overall stability of the sandwich complex.

Figure 10 shows that the electronic structure of $BPY-Ti_2$ is similar to that of $BPY-V_2$. A small difference comes from the fact that Ti−Ti bonding is stronger than V−V bonding in $BPY-V_2$, as indicated by the difference in M−M distances shown in Table 2. In addition, the overlap splitting of bonding and antibonding interactions of d(Ti)-derived levels is larger than that in $BPY-V_2$ because d(Ti) orbitals are spatially more extended than d(V) orbitals. As a result, the spin-polarization of the complex comes from one-half filling of levels derived

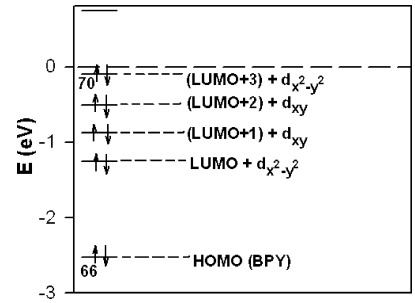

Figure 11. Energy level diagram of $\mathbf{BPY_2-Ti_2}$ sandwich complex.

from $d_{yz}^B(V)$, $d_z2^B(V)$, $d_{yz}^A(V)$, and $d_{xy}^A(V)$, which is responsible for the quintet spin configuration. Figure 11 shows that the electronic structure of BPY_2-Ti_2 is quite similar to that of BPY_2-V_2, except that BPY_2-Ti_2 has two fewer electrons in d_z2-derived levels. As a result, the system exhibits singlet spin configuration.

Finally, we briefly describe our results on the 1D $(BPY-Ti_2)_x$ nanowire. The optimized lattice constant (= 3.61 Å) along the Z direction is slightly larger than that (= 3.42 Å) of $(BPY-V_2)_x$ because the d(Ti) orbitals are spatially more extended than the d(V) orbitals. The lattice energy (= −3.80 eV) is slightly larger than that of $(BPY-V_2)_x$. Our separate analysis on the band structure of the wire (not shown here) indicates that its magnetism also originates from spin-polarization in d_z2(Ti)-derived states. Therefore, the magnetic moment (= 1.73 μ_B) of the system is comparable to that of $(BPY-V_2)_x$. Considering that BPY_2-Ti_2 exhibits no spin-polarization, it is evident that surface effect forces spin-pairing in BPY_2-Ti_2, whereas the bulk environment of the nanowire introduces quite different spin coupling. As an example, we recall that Figure 11 shows that the HOMO of BPY_2-Ti_2, which is derived from an antibonding interaction of two $d_{x^2-y^2}$(Ti) orbitals, interacts with (LUMO+3)(BPY) in the sandwich complex of BPY_2-Ti_2. In the nanowire, however, the Bloch theorem does not allow the $d_{x^2-y^2}$(Ti) orbital to interact with any π(BPY) orbital (including LUMO+3) at the zone boundary. Therefore, the electronic structure of the nanowire should have no direct correlation with that of BPY_2-Ti_2. Its magnetic coupling is similar to that of $(BPY-V_2)_x$ nanowire, noting that local magnetic moments of Ti and BPY are 0.70 and −0.04 μ_B, respectively.

4. Conclusions

Using calculations based on density functional theory, we have investigated geometric, energetic, electronic, and magnetic properties of complexes of BPY with metal atoms M (= Li, V, and Ti). The systems of interest include $BPY-M_2$ and BPY_2-M_2 complexes and 1D $(BPY-M_2)_x$ nanowires. We find that the BPY−Li interaction is purely ionic through charge transfer and that BPY can be a better Li-storage capacitor than naphthalene because it adsorbs Li atoms more strongly.

In contrast, the BPY−V and BPY−Ti interactions are partially covalent, resulting in stronger binding. Consequently, $BPY-Li_2$ adopts an anti configuration, whereas $BPY-V_2$ and $BPY-Ti_2$ adopt syn configurations. The electronic and magnetic properties of the latter complexes can be understood in terms of strong M−M interaction, partially contributed by sd hybridization. Corresponding properties of the BPY_2-V_2 and BPY_2-Ti_2 sandwich complexes can be understood in terms of the much weaker M−M interaction. As can be expected from the rigid charge-transfer model, $(BPY-Li_2)_x$ is a semiconductor with an appreciable band gap, where valence and conduction

bands are nearly flat. In contrast, the $(BPY-V_2)_x$ and $(BPY-Ti_2)_x$ nanowires are metallic because the bands around the Fermi level exhibit appreciable dispersion due to strong hybridization of d(M) orbitals with π(BPY) orbitals. Their magnetic properties can be ascribed to the spin-polarization in d_z2(M)-derived bands.

The major difference between BPY_2-V_2 and Np_2-V_2 sandwich complexes as well as between their nanowires is that the V−V interaction is weaker and V−π(BPY) interaction is stronger in systems involving BPY. As a result, η^6-interaction is stronger, and the $(BPY-V_2)_x$ nanowire is metallic, whereas the $(Np-V_2)_x$ nanowire was known to be half-metallic. We expect that our finding could stimulate further investigations on metal−aromatic complexes and their nanowires as well as their applications in Li storage and nanoelectronics.

Acknowledgment. We thank Jeonju University for financial support.

References and Notes

(1) Vollmer, J. M.; Kandalam, A. K. *J. Phys. Chem. A* **2002**, *106*, 9533.

(2) Kang, H. S. *J. Phys. Chem. A* **2005**, *109*, 478.

(3) Miyajima, K.; Nakajima, A.; Yabushita, S.; Knickelbein, M. B; Kaya, K. *J. Am. Chem. Soc.* **2004**, *126*, 13202.

(4) (a) Ervin, K. M.; Armentrout, P. B. *J. Chem. Phys.* **1985**, *83*, 166. (b) Chen, Y.-M.; Armentrout, P. B. *Chem. Phys. Lett.* **1993**, *210*, 213. (c) Meyer, F.; Kahn, F. A.; Armentrout, P. B. *J. Am. Chem. Soc.* **1995**, *117*, 9740. (d) Jacobson, D. B.; Freiser, B. S. *J. Am. Chem. Soc.* **1984**, *106*, 3900. (e) Hettich, R. L.; Jackson, T. C.; Stanko, E. M.; Freiser, B. S. *J. Am. Chem. Soc.* **1986**, *108*, 5086. (f) Afzaal, S.; Freiser, B. S. *Chem. Phys. Lett.* **1994**, *218*, 254.

(5) (a) Nakajima, A.; Kaya, K. *J. Phys. Chem. A* **2000**, *104*, 176. (b) Miyajima, K.; Muraoka, K.; Hashimoto, M.; Yasuike, T.; Yabushita, S.; Nakajima, A. *J. Phys. Chem. A* **2002**, *106*, 10777.

(6) (a) Hoshino, K.; Kurikawa, T.; Takeda, H.; Nakajima, A.; Kaya, K. *J. Phys. Chem.* **1995**, *99*, 3053. (b) Yasuike, T.; Nakajima, A.; Yabushita, S.; Kaya, K. *J. Phys. Chem. A* **1997**, *101*, 5360.

(7) Kang, H. S. *J. Phys. Chem. A* **2005**, *109*, 9292.

(8) (a) Xiang, H.; Yang, J.; Hou, J. G.; Zhu, Q. *J. Am. Chem. Soc.* **2006**, *128*, 2310. (b) Maslyuk, V. V.; Bagrets, A.; Meded, V.; Arnold, A.; Evers, F.; Brandbyge, M.; Bredow, T.; Mertig, I. *Phys. Rev. Lett.* **2006**, *97*, 097201.

(9) (a) Wang, J.; Acioli, P. H.; Jelinek, J. *J. Am. Chem. Soc.* **2005**, *127*, 2812. (b) Weng, H.; Ozaki, T.; Terakura, K. *J. Phys. Soc. Jpn.* **2008**, *77*, 014301.

(10) Zhang, Z.; Wu, X.; Guo, W.; Zeng, X. C. *J. Am. Chem. Soc.* **2010**, *132*, 10215.

(11) Zhang, X.; Wang, J.; Gao, Y.; Zeng, X. C. *ACS Nano* **2009**, *3*, 537.

(12) (a) Koleini, M.; Paulsson, M.; Brandbyge, M. *Phys. Rev. Lett.* **2007**, *98*, 197202. (b) Zhou, L.; Yang, S.-W.; Ng, M.-F.; Sullivan, M. B.; Tan, V. B. C.; Shen, L. *J. Am. Chem. Soc.* **2008**, *130*, 4023. (c) Wu, J.-C.; Wang, X.-F.; Zhou, L.; Da, H.-X.; Lim, K. H.; Yang, S.-W.; Li, Z.-Y. *J. Phys. Chem. C* **2009**, *113*, 7913. (d) Wang, L.; Cai, Z.; Wang, J.; Lu, J.; Luo, G.; Lai, L.; Zhou, J.; Qin, R.; Gao, Z.; Yu, D.; Li, G.; Mei, W. N.; Sanvito, S. *Nano Lett.* **2008**, *8*, 3640.

(13) Kurikawa, T.; Takeda, H.; Hirano, M.; Judai, K.; Arita, T.; Nagano, S.; Nakajima, A.; Kaya, K. *Organometallics* **1999**, *18*, 1430.

(14) (a) Kresse, G.; Hafner, J. *Phys. Rev. B* **1993**, *47*, 558. (b) Kresse, G.; Joubert, D. *Phys. Rev. B* **1999**, *59*, 1758.

(15) Kresse, G.; Furthmüller, J. *Phys. Rev. B* **1996**, *54*, 11169.

(16) Perdew, J. P.; Burke, K.; Ernzerhof, M. *Phys. Rev. Lett.* **1996**, *77*, 3865.

(17) Almenningen, A.; Bastiansen, O. *K. Nor. Vidensk. Selsk.* **1958**, *4*, 1.

JP110442X